

USING FRACTALS TO DETERMINE A RESERVOIR'S HYDROCARBON DISTRIBUTION

Steve Cuddy

Copyright 2017, held jointly by the Society of Petrophysicists and Well Log Analysts (SPWLA) and the submitting authors.
This paper was prepared for presentation at the SPWLA 58th Annual Logging Symposium held in Oklahoma City, Oklahoma, USA, June 17-21, 2017.

ABSTRACT

To determine a field's hydrocarbon in place, it is necessary to model the distribution of hydrocarbon and water throughout the reservoir. A water saturation vs. height (SwH) function provides this for the reservoir model. A good SwH function ensures the three independent sources of fluid distribution data are consistent. These being the core, formation pressure and electrical log data. The SwH function must be simple to apply, especially in reservoirs where it is difficult to map permeability or where there appears to be multiple contacts. It must accurately upscale the log and core derived water saturations to the reservoir model cell sizes.

This paper clarifies the, often misunderstood, definitions for the free-water-level, transition zone and irreducible water saturation. Using capillary pressure theory and the concept of fractals, a practical SwH function is derived. Logs and core data from eleven fields, with very different porosity and permeability characteristics, depositional environments and geological age, are compared. This study demonstrates how this SwH function is independent of permeability and litho-facies type and accurately describes the reservoir fluid distribution.

The shape of the SwH function shows that of the transition zone is related more to the fractal pore geometry rather than porosity or permeability alone. Consequently, this SwH function gives insights into a reservoir's quality as determined by its pore architecture. Several case studies are presented showing the excellent match between the function and well data. The function makes an accurate prediction of water saturations, even in wells where the resistivity log was not run due to well conditions.

The function defines the free water level, the hydrocarbon to water contact, net reservoir cut-off, the irreducible water saturation and the shape of the transition zone for the reservoir model. The function provides a simple way to quality control electrical log and core data and justifies using core plug sized samples to model water saturations on the reservoir scale.

INTRODUCTION

Water saturation vs. height (SwH) functions are required to initialise a 3D static and dynamic reservoir model with the water and hydrocarbon volumes, to pick fluid contacts and the net reservoir cut-off.

Figure 1 shows a typical reservoir model. It has cells where the colour represents porosity, permeability and/or facies type. The lines are wells where electrical log and core data are collected. These limited data are used to populate the reservoir model.

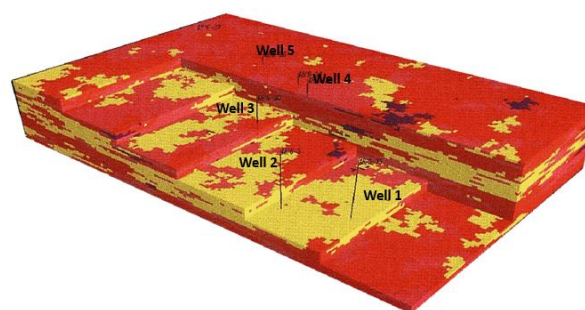


Figure 1: Typical 3D Reservoir Model

WATER SATURATION VS. HEIGHT FUNCTION

The SwH function describes how water saturation varies with height above the free water level (FWL).

Water saturation (Sw) determined from interpretation of log and core data can only represent the reservoir within a few feet surrounding the well bore. Sw cannot be mapped as it depends on numerous factors including porosity and the height above the local FWL.

SwH functions are used in a field's reservoir model to determine Sw away from well locations so that hydrocarbons initially in place can be calculated. The error in reserves resulting from an equation that poorly describes the reservoir can be significant.

The Saturation Height Function, as shown by Figure 2, tells us how water saturation varies as a function of the height above the Free Water Level. It also tells us how the formation porosity is split between hydrocarbon and water; and the shape of the transition zone. It is used to populate and initialize the 3D reservoir model.

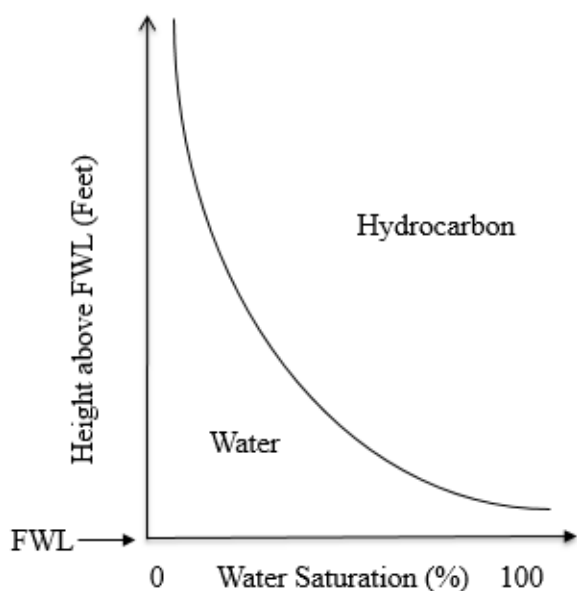


Figure 2: Water Saturation vs. Height Function

A good SwH function requires three independent sources of fluid distribution data are consistent.

These are:

- Formation pressure data
- Electrical log data
- Core data

The function must account for varying permeability and fluid contacts throughout the field. It must upscale correctly from the core plug scale and ½ foot logging scale to the reservoir model cells scale and should be easy to apply.

THE FREE WATER LEVEL

The Free Water Level (FWL) is the horizontal surface of zero capillary pressure as shown in Figure 3. The FWL is the level formation fluids would separate out in a very wide borehole. It is the intersection point of hydrocarbon and water pressures on a formation vs. true vertical depth plot. The formation fluid pressures form linear lines, even in the transition zone as the formation pressure tool only responds to the mobile fluid phase, as explained later. The FWL is the start point for SwH plot, but only for very high porosities.

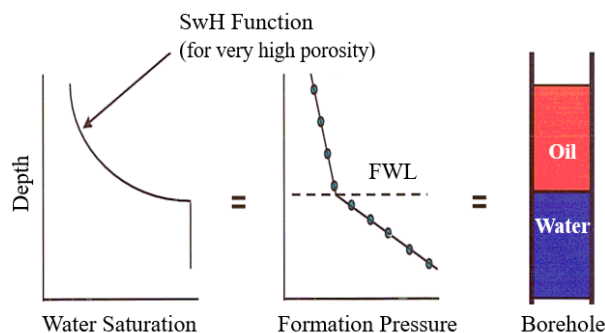


Figure 3: The Free Water Level

THE HYDROCARBON WATER CONTACT

The Hydrocarbon Water Contact (HWC) is shown by Figure 4, is the height where the pore entry pressure is sufficient to allow hydrocarbon to start invading the formation pores. This depends on the local porosity & permeability. It is a surface of variable height.

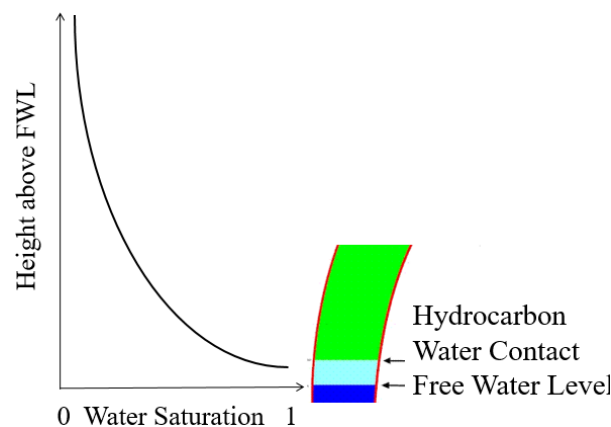


Figure 4: The Hydrocarbon Water Contact

THE BULK VOLUME OF WATER

The Bulk Volume of Water (BVW) is the proportion of water in a unit volume of reservoir rock as shown by Figure 5. The blue shows the proportion of pore space filled with water. BVW is simply the product of porosity and water saturation. BVW is what is measured with resistivity tools in clean formation, not Sw but the conductivity of the water *volume*. This is what is measured by core analysis, not Sw but the *volume* of water displaced.

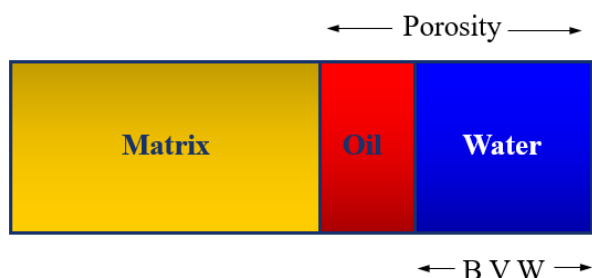


Figure 5: The Bulk Volume of Water (BVW)

FRACTALS AND RESERVOIR DESCRIPTION

Fractals are mathematical objects for which their parts are identical to the whole set, except for a change of scale. Other names for fractals are self-similarity or scale invariance.

Detailed studies of the fractal modelling of reservoirs were undertaken by Al-Zainaldin, Glover and Lorinczi, who kindly discussed with the author their understanding of the fractal modelling of reservoirs. It has been shown that sandstones have fractal geometric pore spaces (Katz and Thompson 1985). Fractals are very useful since they can describe the broad range of variability which exists in reservoir properties including grain-size, porosity and permeability (Perez and Chopra 1997).

The fractal concept as suggested by Mandelbrot (1977) has found various applications throughout the geosciences. This is because many physical systems in nature produce a variation of properties that can be described by fractals (Lozada-Zumaeta et al. 2012). Several studies have been made relating the fractal theory to the distribution of reservoir properties. Turcotte (1997) modelled the sedimentation process by the Devil's Staircase, which is an exact fractal, and showed that the rate of sedimentation can be related to the time interval of deposition occurrence by a fractal power law relationship.

Since the formation of porosity is closely linked to both sedimentation processes and to fragmentation, both of which show fractal behaviour, it follows that porosity would be expected to follow a fractal behaviour too. In other words, if the grain size distribution is fractal, then the pore size would also be expected to be distributed fractally. Laboratory measurements have confirmed that the porosity of sandstones is indeed fractal, exhibiting a non-integer power law scaling behaviour, as will be explained later.

The statistics of sediment distribution is controlled by the natural processes which created them. Since these processes have been proven to behave fractally, it is expected that the distribution of sediments will show fractal behaviour too. (Al-Zainaldin, Glover and Lorinczi 2016).

A fractal image is shown by Figure 6. It may look complex but is based on a very simple repeating pattern.

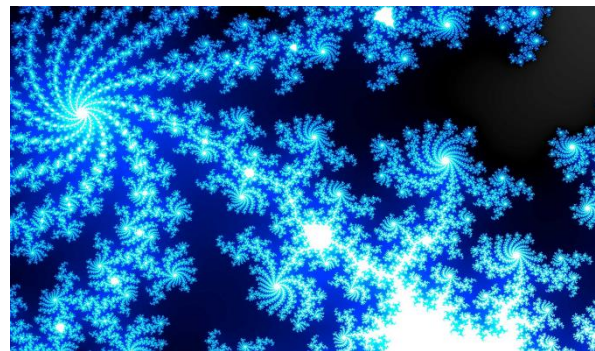


Figure 6: Fractal Image

Fractals are found throughout nature, in the Cosmic Microwave Background (CMB) shown by Figure 7. These patterns of slight variations in temperature, from the early universe, go on to give rise to the galaxies and galactic superclusters each with similar structures.

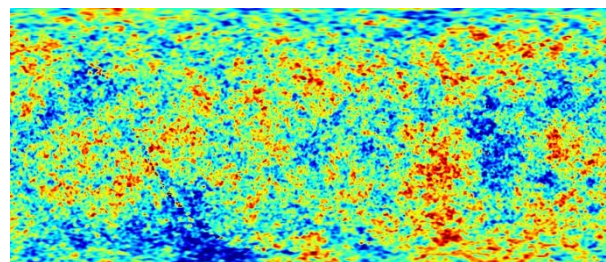


Figure 7: The Cosmic Microwave Background

Figure 8 shows the Himalayas mountain range as seen from space. The patterns seen in the mountain range are repeated as you zoom in on the main valleys and the valleys that branch off them.



Figure 8: The Himalayas as seen from Space

The snowflake, shown in Figure 9 is a fractal object.



Figure 9: Snowflake

Fractals are never-ending patterns. Fractals are infinitely complex patterns that look the same at every scale, that are created by a simple repeating process. Benoit B. Mandelbrot (1977) coined the word Fractal. The Mandelbrot pattern shown in Figure 6 is created by the recursive formula:

$$Z_n = Z_{n-1}^2 + \text{Constant} \quad \text{Equation 1}$$

Fractals are objects where their parts are identical to the whole, except for scale as shown by the tree in Figure 10.



Figure 10: Fractals shown in a Tree

From a distance the overall pattern of a tree can be seen to consist of a trunk and the main branches. On closer inspection, the smaller branches show the identical pattern. Even the twigs show the same pattern.

This is why nature can create many complex organisms through a simple fractal repeating process. As a consequence, many complex objects may be described by fractals.

FRactal Dimensions

The origin of the term Fractal is due to the fact that they have a fractional dimension, not a whole number value. Whereas classical geometry deals with objects of integer dimension, fractal geometry describes non-integer dimension. Points have zero dimension, lines and curves have one dimension, squares and circles have two dimensions and cubes and spheres have three dimensions.

If we increase the side of a cube by a factor of 3 the 2D area of the cube's side increases by a factor of 9 and cube's volume increases by a factor of 27. This relationship is given by the Equation 2.

$$N = r^D \quad \text{Equation 2}$$

where D is the dimension, r the length of the side of the object and N is the number of the units (with a side of r) that will fill entire object.

If we measure the increase in a reservoir property such as porosity with the decrease of the measuring metric, this will give the dimension D . The dimension D need not be an integer, as it is in Euclidean geometry, has it could be a fraction. This is why it known as fractal geometry.

The fractal dimension is a representation of the heterogeneity of the fractal object. Greater the dimension, the more heterogeneous the fractal object (Li 2004).

FRACTAL GEOMETRY OF PORE SPACE

We assume that pore network of a rock sample is made up of N pore tubes with the same length but different radii. This capillary tube model is used in the Washburn equation to calculate the pore size distribution of a rock sample from mercury injection capillary pressure data (Mandal 2006).

Therefore, from the capillary tube model, unit area (A) of rock sample can be represented by:

$$A = N(r).r^2 \quad \text{Equation 3}$$

Substituting Equation 2 into Equation 3:

$$A = r^{(2+D)} \quad \text{Equation 4}$$

The volume of the model is:

$$V = r^{(3+D)} \quad \text{Equation 5}$$

QUANTIFYING FRACTAL GEOMETRY

We use the example of a coastline, as shown in Figure 11, to mathematically confirm and qualify fractal behaviour.

If we ask, "How long is the coast of Great Britain," the answer is that it depends on how closely you look at it, or how long your measuring stick is. As shown by Figure 12, the length Great Britain's coastline (N) depends on the length of your ruler (r) where r is the magnification of the ruler.¹



Figure 11: The Coastline of Great Britain

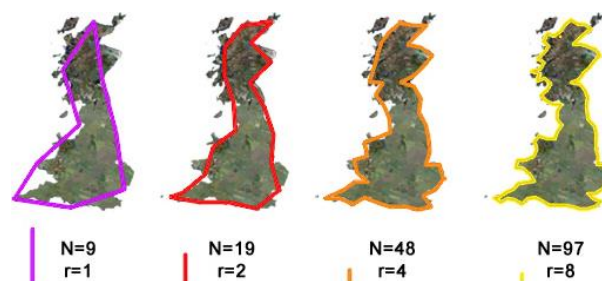


Figure 12: The Coastline of Great Britain at using different rulers

When we use a large ruler ($r=1$, a small magnification factor), we get a very poor approximation, shown in purple, and a value for the coastline of $N=9$. As the ruler length shrinks, the magnification r increases, and the value of the coastline N increases. We are interested in the *rate* at which the coastline changes as a function of the ruler length. The curvier the coastline is, the more the coastline will increase as the ruler shrinks.

To understand the relationship, we plot the coastline versus the magnification factor (or the inverse of the ruler length) using logarithmic scales, as shown by Figure 13. As the ruler shrinks the measured coastline increases. If the coastline is fractal the relationship between r and N is *linear* when plotted using log scales, which is the case for the coastline of Great Britain.

¹ Fractalfoundation.org

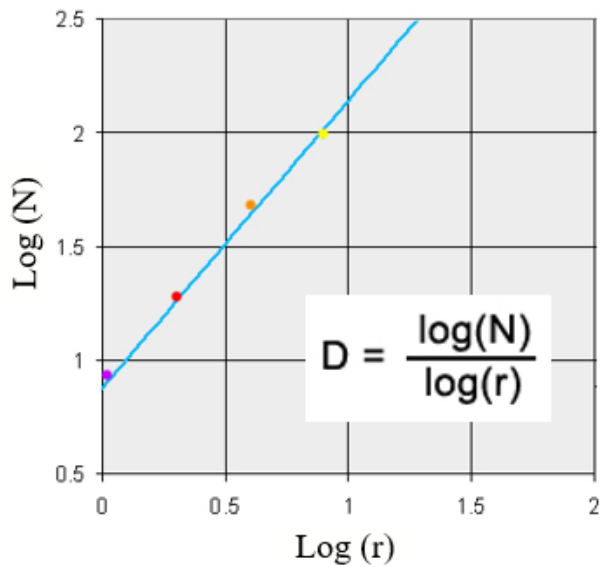


Figure 13: Plot of Ruler Length vs. Coastline Length

D is the fractal dimension and the colour of the points referred to Figure 12.

FRACTAL BEHAVIOUR IN RESERVOIR ROCKS

Reservoir rocks can be shown to be fractal by using a box counting method analogous to the measuring method we used for the coastlines. But in this case, we cover the image with a grid, and then count how many boxes of the grid are covering part of the image. Then we do the same thing but using a finer grid with smaller boxes. By shrinking the size of the grid (i.e. by increasing the magnification) we can more accurately measuring the porosity as shown by Figure 14.

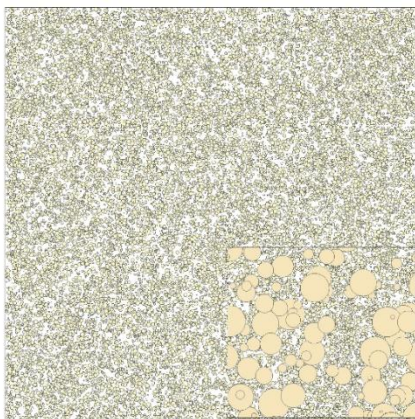


Figure 14: Pore Structure at Increased Magnification

To study the pore structure of the rock samples, specimens are first saturated with a blue-dyed epoxy.

Thin sections were then imaged with a scanning electron microscope (SEM). The method involves counting the number of pixel units representing porosity at different magnifications.

The fractal nature of Berea Sandstone shown by Figure 15 which shows a linear relationship between the pixel size and the number of pixels representing porosity in the thin sections.

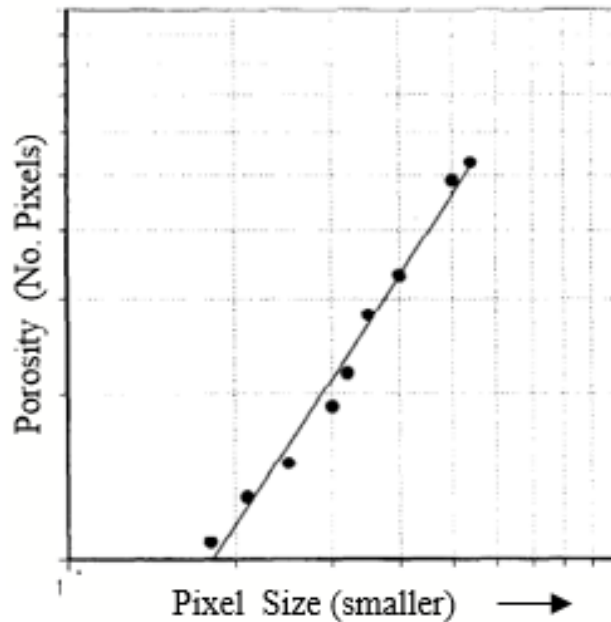


Figure 15: Fractal Nature of Berea Sandstone

The smaller the pixel size more porosity is identified in the smaller pores and in the pore throats. The linear relationship (on logarithmic scales) show the Berea sandstone is fractal in nature.

BUOYANCY FORCES IN RESERVOIR FLUIDS

When a field is originally deposited, the structure usually contains water. When hydrocarbons migrate into a trap, the buoyancy force exerted by the lighter oil (or gas) will push the water that was previously in the pore space downward. However, not all of the water is displaced; some of it will be held by capillary (electrostatic) forces within the pores. Narrower capillaries, pores with smaller pore throats, with the larger surface area, hold onto the water the strongest.

As shown by Figure 16 , the water at a given height in a reservoir is determined by the balance between the capillary forces holding the water up and the force of gravity pulling the water down.

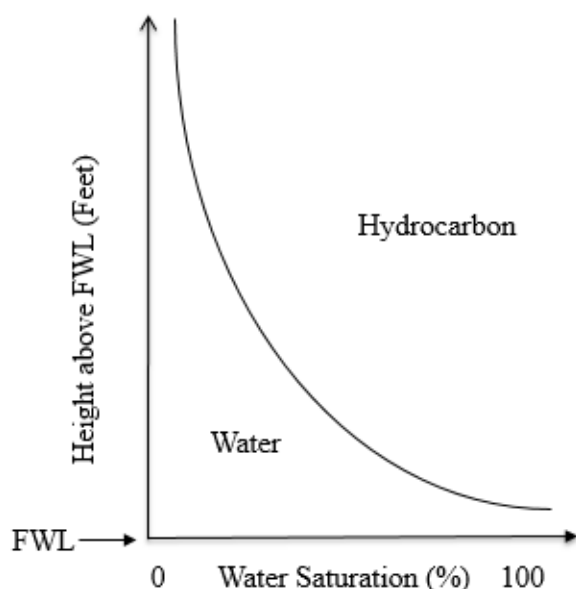


Figure 16: The division of pore space as a function of height for a fixed porosity.

The oil (or gas) is the *mobile* phase and only enters the space not occupied by water in the reservoir pores. Therefore, a given part of the pore space within the reservoir will contain both oil and water. The percentage of water in the pore space is known as the water saturation (S_w).

CAPILLARY PRESSURE

When two fluids meet in a capillary tube there is a difference in pressure across their interface. This "Capillary Pressure" is caused by the preferential wetting of the capillary walls by the water and gives rise to the familiar curved meniscus and causes the water to rise up the capillary as shown by Figure 17.

The capillary pressure characteristics of reservoir rocks affects the distribution of fluids within the reservoir. It is one of the most important measurements that can be made because it relates reservoir rock and reservoir fluid properties. The magnitude of capillary pressure reported in laboratory measurements relates to the height above the free water level in the reservoir.

The relationship between capillary pressure and water saturation is dependent upon grain size, grain shape, packing, sorting and cementation (environment of deposition and diagenesis). These all affect the pore throat diameter distribution, often referred to as the pore size distribution (PSD) within the rock. The relationship is also dependent upon the interfacial tension between

the two immiscible phases present, the contact angle between the wetting phase, the rock surface and the density difference between the fluids.

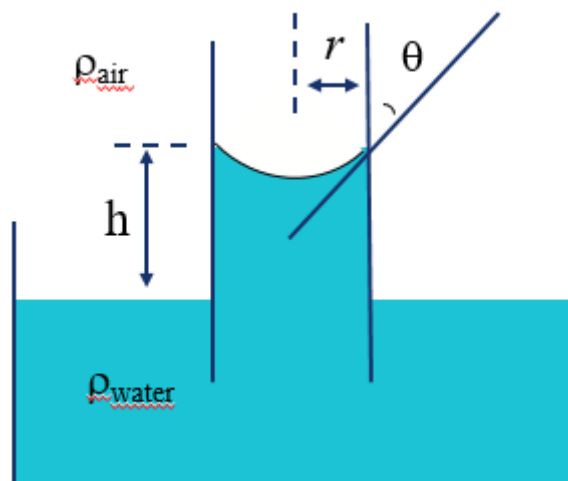


Figure 17: Capillary pressure draws up and holds the water

Capillary pressure curves can be defined for any two-phase system in a given rock. All that will vary is the interfacial tension and the contact angle. It is therefore possible to convert one capillary pressure curve to another, provided the relevant values of interfacial tension and contact angle are known.

The height of the water in a capillary depends on the capillary pressure, which is determined by the radius of the capillary and the fluid types. The relationship between capillary pressure and pore size is the Young-Laplace equation shown by Equation 6.

$$P_C = \frac{2\sigma \cos(\theta)}{r} \quad \text{Equation 6}$$

Where:

P_c capillary pressure
 r capillary radius
 σ interfacial tension
 θ contact angle

Consequently, smallest pores hold on to the most water as shown by Figure 18.

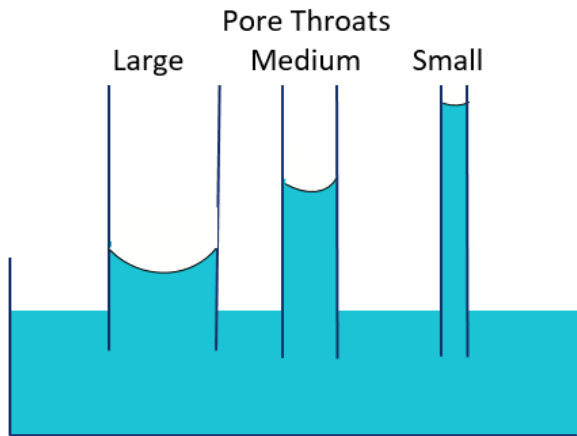


Figure 18: Smallest pores hold the most water

Substituting Equation 6 into Equation 5

$$V = aP_c^{(D+3)} \quad \text{Equation 7}$$

Where a = constant

As the capillary pressure only acts on the water phase, the volume V can be replaced by the Bulk Volume of Water (BVW)

$$BVW = aP_c^b \quad \text{Equation 8}$$

Where $b = D + 3$

Remember the dimension D is fractal and not necessarily an integer.

THE FORCES ACTING ON RESERVOIR FLUIDS

The force of gravity on the column of water is determined by the difference between the water and oil densities and is called the buoyancy pressure P_b and is given by

$$P_b = (\rho_w - \rho_o)gH \quad \text{Equation 9}$$

Where:

- P_b buoyancy pressure due to gravity
- ρ_w water density
- ρ_o oil density
- g acceleration of gravity
- H height above the free water level (FWL)

Notice that the greater the density difference, the greater the gravity force. The buoyancy pressure is shown in Figure 19.

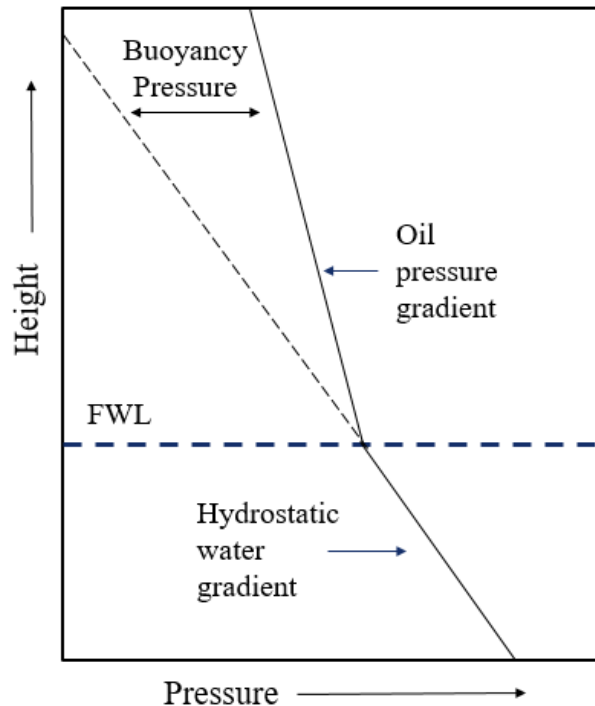


Figure 19 The capillary and gravitational forces acting on the reservoir fluids

The capillary-bound water comprises a continuous column of water within the oil leg, with a hydrostatic pressure gradient. The oil located in the remaining pore space also as a continuous phase but will have a lower pressure gradient.

Although oil and water can coexist in the same localized volume of rock, the pressures acting on the two fluids are very different. The dotted line represents the water gradient which continues into the water leg. The solid line above the FWL is the oil gradient. The formation pressure tester tool measures the mobile phase shown by the solid line. The intersection of the pressure gradients indicates the free water level (FWL), as shown by the dashed line.

The buoyancy pressure (the difference in pressure between the oil and water phases) increases with height above the FWL. As the buoyancy pressure increases the oil phase will displace more water from increasingly smaller pore volumes. Most water is held in the smallest pores closest to the FWL. Therefore, S_w will *tend* to decrease with height above the FWL, but is not always the case as will be shown later.

The volume of water remaining at a given height in a reservoir is a function of the balance of capillary forces

holding up the water up and the force of gravity acting together with the density contrast between the reservoir fluids, acting to pull the water down.

The balance between capillary pressure and the buoyancy pressure is:

$$P_c = P_b \quad \text{Equation 10}$$

From Equation 9 above

$$P_c = P_b = (\rho_w - \rho_H)gH \quad \text{Equation 11}$$

Rearranging this Equation, we get

$$H = \frac{P_c}{(\rho_w - \rho_H) \bullet g} \quad \text{Equation 12}$$

P_c and H are interchangeable as a function of the reservoir fluids

From Fractals Equation 7

$$BVW = aP_c^b \quad \text{Equation 13}$$

As P_c can be replaced by H

$$BVW = aH^b \quad \text{Equation 14}$$

The constant ' b ' is dimensionless. Consequently, the equation is independent of scale and applies to core plugs as well as the entire reservoir.

This equation has been called the Fractal (or FOIL) Function and describes the variation of BVW as a function of the Height above the Free Water Level (Cuddy 1993).

SOUTHERN NORTH SEA GAS FIELD STUDY

Figure 20 shows the water saturation vs. height above the FWL data from a large Southern North Sea field (Cuddy 1993). The excellent quality dune sands are shown in red, the medium quality sandy sabkhas in blue and the poor fluvial sands in green. The highest porosities, to the left of the plot, give the lowest water saturations, as you would expect. Where the rock is less than 12 p.u. the formation is fully water saturated for hundreds of feet about FWL as shown on the right of the plot.

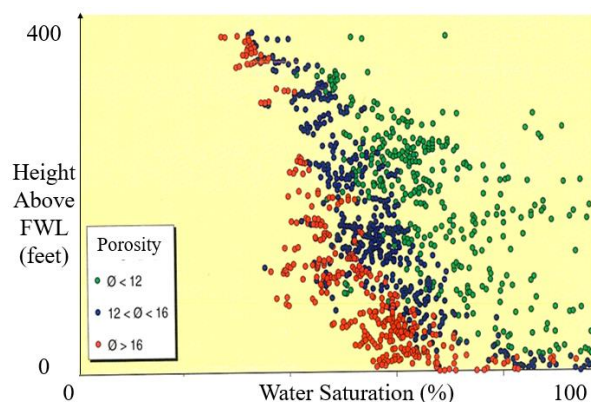


Figure 20: Water Saturation vs. Height above the FWL for a Southern North Sea Gas Field

There is considerable scatter in the data. It is normal practice to divide the data into porosity bands and fit SwH lines.

Deriving the functions for these porosity bands can be very difficult. The SwH curves, by porosity band, derived from this dataset, are shown by Figure 21. The highest porosity band is the bottom left. The lowest porosity band is upper right. These curves are mathematically and visually unconvincing as they *cross*. Also, there is insufficient data in some of the porosity bands to fit the lines. To fit the lines, it is necessary to know the pore entry pressure, also known as the threshold height, which represents the point where the porosity band line meets the right-hand y-axis. Clearly it is not easy to determine this intercept point.

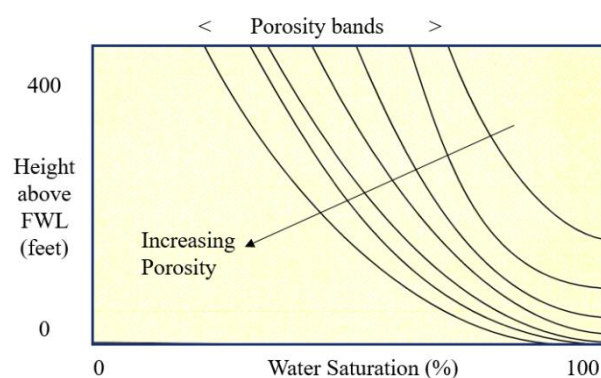


Figure 21: Classical Sw-height Curves by Porosity Band

If we replace Sw in the x-axis by BVW the data collapses as shown by Figure 22.

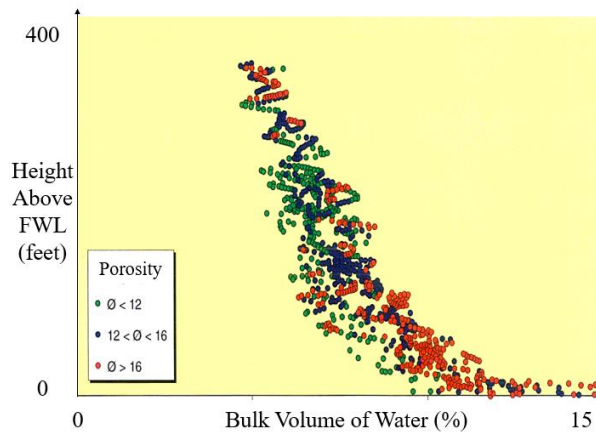


Figure 22: Bulk Volume of Water vs. Height above the FWL for a Southern North Sea Gas Field

This collapse demonstrates the bulk volume of water is independent of porosity, as the porosity points show *no* separate banding as seen in Figure 20. It can easily be shown that the data clusters are independent of other rock parameters, such as permeability or facies type by simply plotting them, in colour, on the z-axis on the cross-plot.

Figure 22 is telling us something very important about the reservoir. The formation water which was there first and is now capillary bound and claims part of the porosity space. At a particular depth in the reservoir the BVW is determined by its height above the FWL. If the porosity is 10 p.u. the hydrocarbon enters the remaining space. If the porosity is 20 p.u., the BVW is the same, but extra available porosity is filled with hydrocarbon. This is shown by Figure 23.

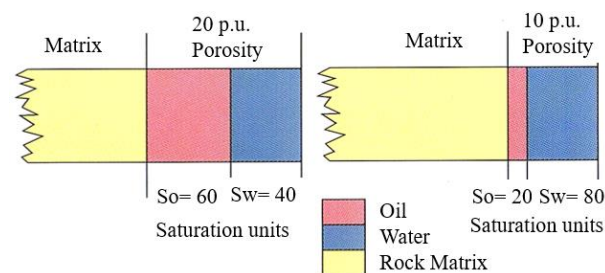


Figure 23: Bulk Volume of Water as a function of height

In this case, with BVW is the same at 9 p.u., but S_w increases from 40% to 80% as the porosity decreases from 20 p.u. to 10 p.u.

NET RESERVOIR

'Net Reservoir' are intervals of rock that is capable of holding hydrocarbon. This should not be confused with 'Net Pay' which is the ability of the reservoir to produce hydrocarbons. Knowledge of what is net reservoir is essential for upscaling parameters, including porosity and water saturation and for calculating hydrocarbon in place from the reservoir model. The net reservoir cut-off *varies* as a function of height above the FWL as shown by Figure 24.

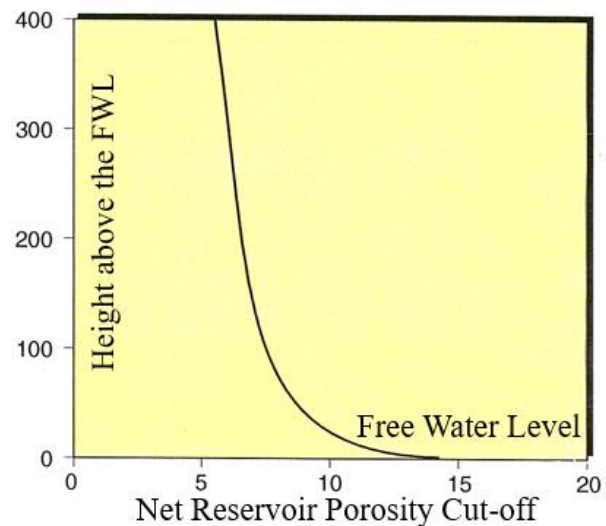


Figure 24: Net Reservoir varying as a function of height above the FWL

Reservoir high above the FWL has low saturations of capillary bound water and hydrocarbon enters the smaller pores. Reservoir just above the FWL contains high saturations of capillary bound water and there is a little room left for hydrocarbons.

This is shown in Figure 25. Net = 1 at 150' whereas Net = 0 at 280', just above the FWL, even though the porosity is higher at 280'.

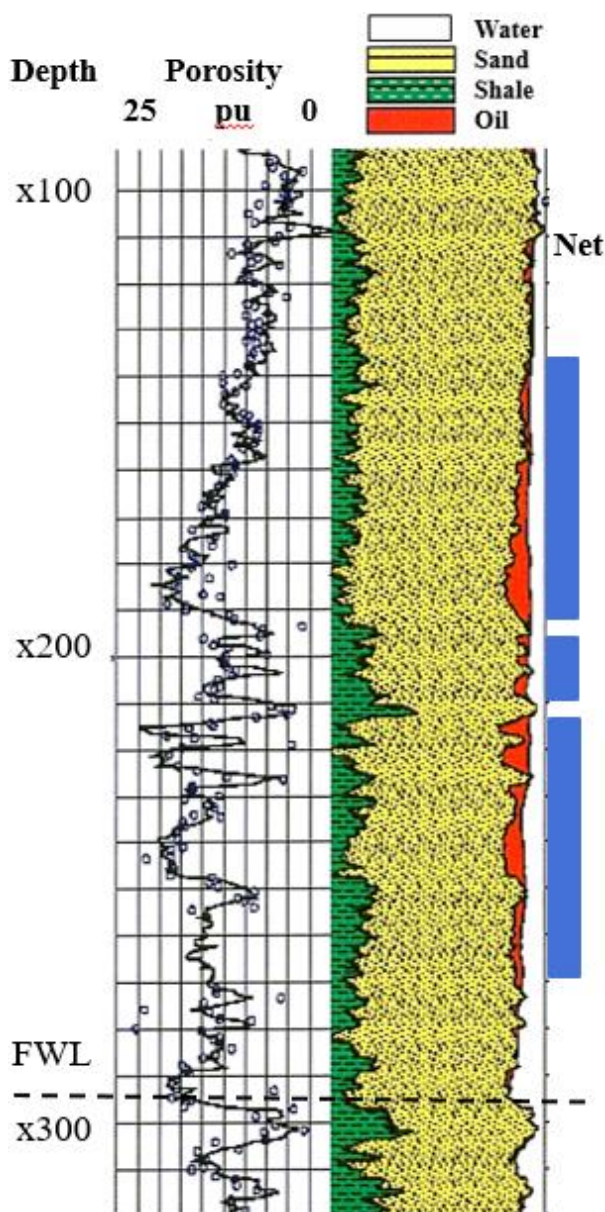


Figure 25: Net Reservoir Case Study

THE FRACTAL FUNCTION

From above the Fractal Function describes the variation of BVW with height above the FWL and is given by:

$$BVW = aH^b \quad \text{Equation 15}$$

Where:

BVW = Bulk Volume Water

H = Height above FWL

a, b = Constants

This function is shown by Figure 26. It is no surprise that this is similar to Figure 24 where the Net Reservoir Cut-

off is replaced by the Bulk Volume of Water. Note that the function is field specific to be determined by electrical log and core data, as explained later.

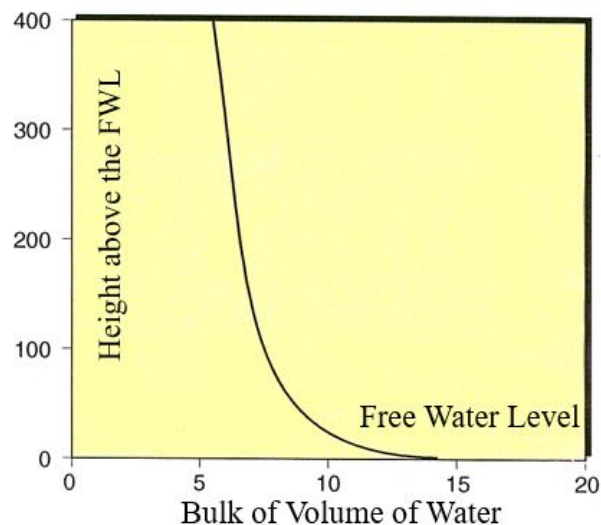


Figure 26: Fractal Function of BVW vs. Height above the FWL

The function has only two parameters and is used in the 3D reservoir model. It has several other important uses as will be described next.

PICKING THE FREE WATER LEVEL

The fractal SwH function points to the Free Water Level as shown for a North Sea oil field as shown by Figure 27 (from Kay 2002). The BVW is plotted against the True Vertical Depth Subsea for two wells which don't intercept the FWL. The BVW trend identifies the FWL at 10,730 ftTVDss and confirms the wells are probably in the same reservoir compartment.

One of a field's main uncertainties is *depth* or more precisely the *true vertical depth* below datum in the reservoir model. The combination of logging depth and deviation survey errors can give an error bar to the TVD depth of +/- 30 feet. This error seriously influences the volumetric computation of the hydrocarbon in place and may even suggest wells are in different fluid/pressure compartments, which would affect the field's development plan. The fractal function can be used to normalise the TVD depths between wells. If the field's formation pressures, geochemical fluid analysis and/or geophysical mapping suggests that wells are in the same compartment - the wells when plotted as shown in Figure 27 can be shifted to a common FWL.

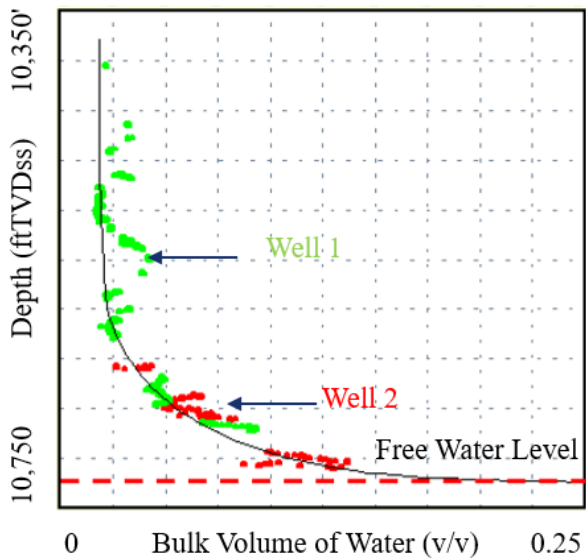


Figure 27: Fractal Function points to the Free Water Level

CALCULATING THE FRACTAL FUNCTION

The BVW function shown in Equation 15 is a straight line when plotted on log scales.

$$\log BVW = \log a + b \log H \quad \text{Equation 16}$$

which is the form of the straight-line equation $y = mx + c$, where 'c' is the intercept of the line with the y-axis and 'm' is the line's gradient. The line is determined by least squares regression, where the predicted variable (BVW) is x-axis (i.e. XonY), rather than the y-axis which is the usual case. Only two valid core or electrical log data points are required to calculate the constants 'a' (from 10^c) and 'b' (gradient m which is negative).

Figure 28 shows the Fractal Function derived from core data for six North Sea fields discussed later in this paper. Notice how the gradient is constant for each of these fields. Consequently, only 2 data points are required to compute the intercept and gradient for each of these core data sets. The author is not recommending that only 2 data points are taken in a field, rather that only the best core data, unaffected by measurement error or core sample fractures are used. The other good data points should be used to confirm the regression line.

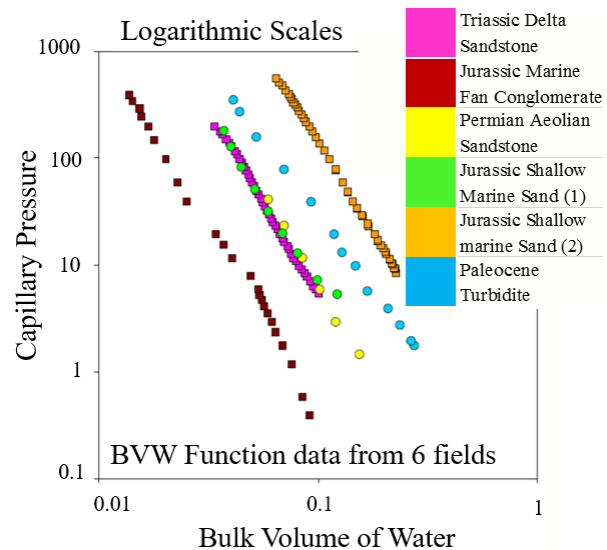


Figure 28: Fractal Function derived from Core Data

A similar argument is used later for electrical log data, where only the best data points from the centre of thick beds are required to determine the fractal function. Consequently, it is not necessary to correct the resistivity log for thin beds, bed boundary effects or conductive shales.

DERIVING WATER SATURATION AND THE HYDROCARBON TO WATER CONTACT

By definition.

$$S_w = \frac{\text{Bulk Volume of Water}}{\text{Porosity}} \quad \text{Equation 17}$$

From Equation 15

$$S_w = \frac{aH^b}{\text{Porosity}} \quad \text{Equation 18}$$

Where:

H = Height above FWL

a, b = Constants

By simply dividing the fractal function by the porosity, the water saturation can be computed in individual wells or in the reservoir model. The Fractal S_wH function gives the Hydrocarbon Water Contact (HWC) as a function of porosity as shown by Figure 29.

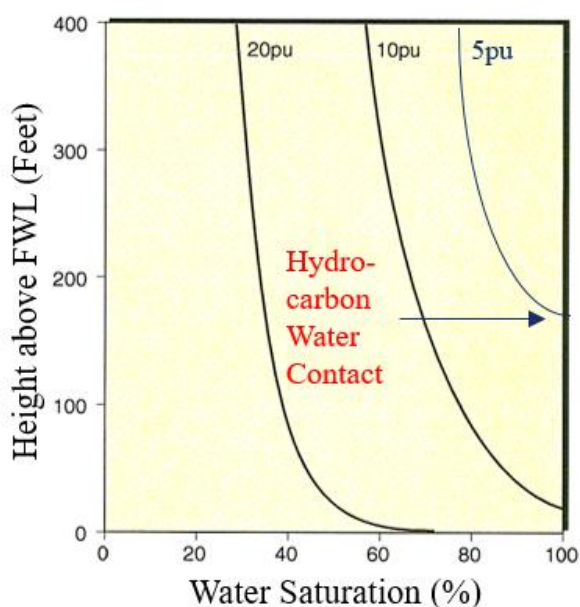


Figure 29: Deriving Sw and the HWC

The HWC depends on the local porosity. In the example shown in by Figure 29 the reservoir rock is fully water saturated for a least 180 feet above the FWL when the porosity is 5 p.u. or less. Note that the Free Water Level (FWL) is the same irrespective of the porosity.

IRREDUCIBLE WATER SATURATION

The Irreducible Water Saturation (S_{wirr}) is the lowest Sw that can be achieved in a core plug by displacing the water. This is achieved by flowing hydrocarbon through a sample or spinning the sample in a centrifuge which depends on the drive pressure or the centrifuge speed.

This is equivalent to moving higher above the FWL. Sw therefore depends on the height above the free water level and the transition zone therefore extends indefinitely. Capillary pressure theory tells us that a minimum irreducible Sw does not exist, as Sw depends on the height and local porosity in the reservoir, as shown by Figure 30.

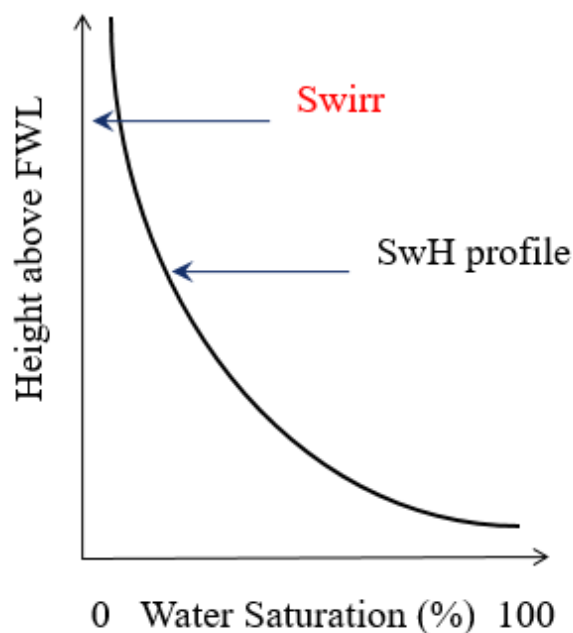


Figure 30: Irreducible Water Saturation

HETEROGENEOUS RESERVOIR CASE STUDY

Figure 31 shows a highly heterogeneous reservoir. The logs and core show large variations in porosity and permeabilities. Consequently, the computed water saturation also shows large variations. Unusually water saturation reduces with height in this well. It would be very difficult to derive SwH Function for these data using conventional methods of porosity banding.

Notice that BVW, shown in white in Track 4, is a simple function of height. The log derived Sw, from the resistivity log, is shown in black in Track 1. The SwH function is shown in red, in Track 1, which is an excellent match. Permeability is not required for this function as the SwH simple function of just two variables; height and porosity.

Only two data points, taken from the thick intervals in the best wells in the field, are required to compute the water saturation. Consequently, the fractal SwH function downgrades resistivity logs in later wells from being 'essential' to 'nice to have'. In addition, only the very best resistivity log is required to derive the function. Consequently, thin bed effects, bed boundary effects and shale effects, can be ignored.

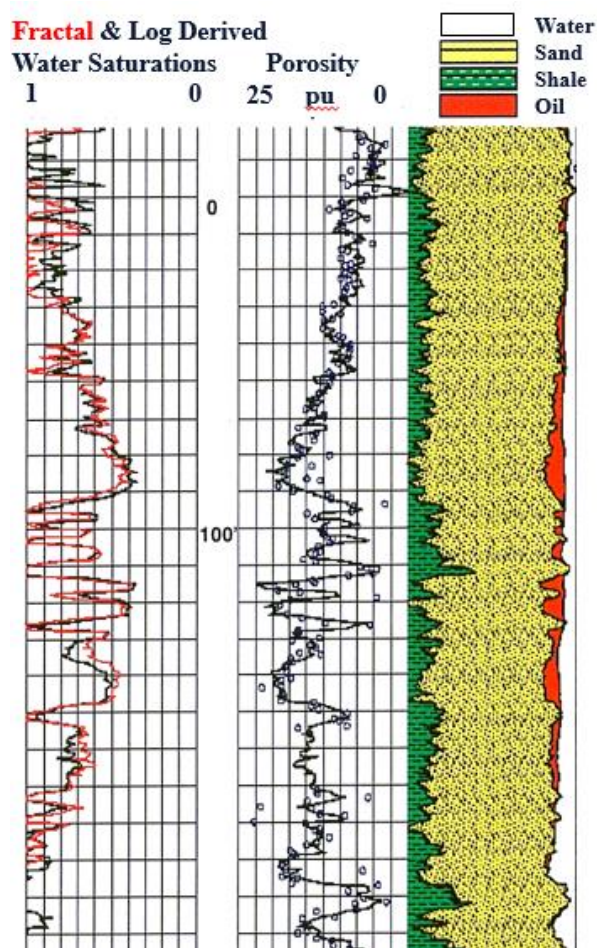


Figure 31: Fractal Case Study

CORE WATER SATURATIONS

In order to confirm that the Fractal SwH Function correctly predicts Sw, an independent source of Sw is required for comparison. Core derived Sw is an excellent independent source of Sw. Accurate water saturations can be derived from core if taken from wells drilled with oil base mud which has being 'doped' to identify any mud filtrate contamination. Only the centre of cores taken above the FWL, where the capillary bound water is immobile, are sampled.

Figure 32 shows the comparison between water saturations determined from the resistivity log (black line), the fractal function (red line) and core (blue dots). The core confirms the water saturations determined by fractal function.

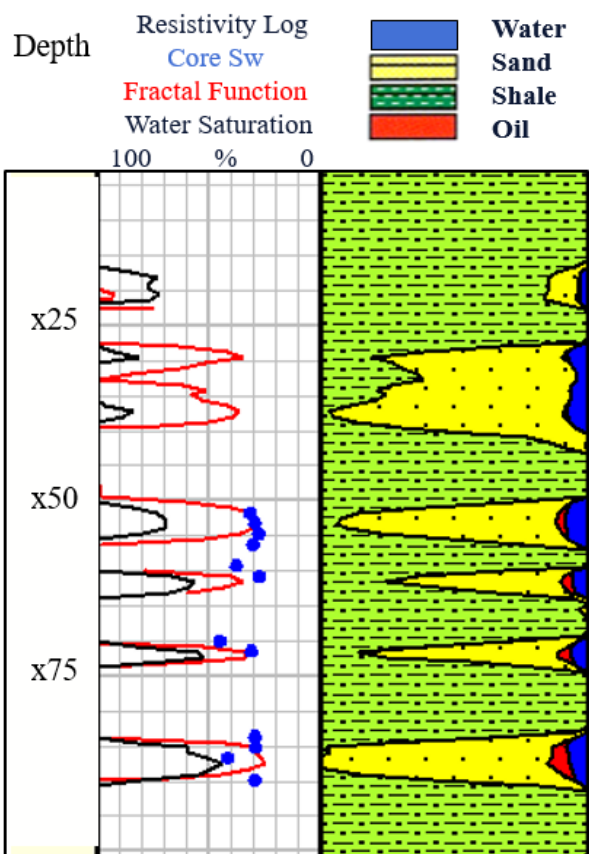


Figure 32: Core Water Saturations

Consequently, it is not necessary to correct the resistivity log for the thin bed effects.

SWEPT AND BY-PASSED HYDROCARBON

Figure 33 shows a well from Heather oil field located in the Northern North Sea, where oil is produced from sandstones of the Middle Jurassic Brent Group (Kay 2002).

Track 1 shows the water saturation determined from the resistivity log (black) and the fractal function (purple). Tracks 2 and 3 shows the computer processed well interpretation using the resistivity and fractal function respectively. The water saturations agree in the thick beds except between 100 and 120 ft. As the fractal function gives the initial oil in place and the resistivity log the water saturations at the time of logging, the difference shows a depleted zone and the value for the residual Sw.

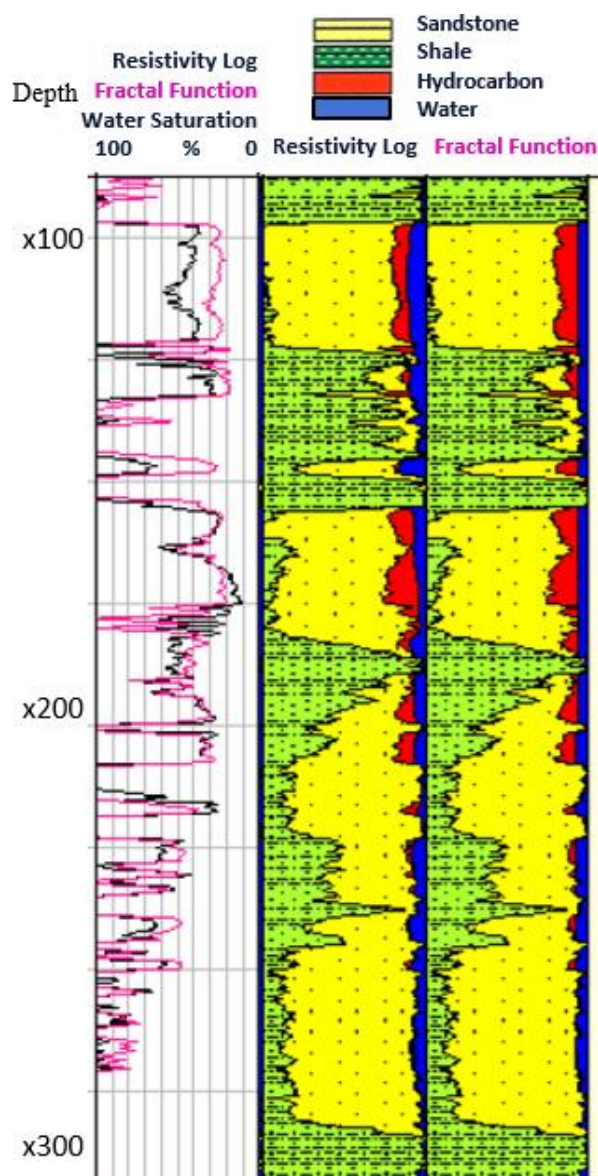


Figure 33: Hydrocarbon swept and by-passed zones

In contrast the interval between 160 and 175 ft shows similar Sw. Consequently, this has been interpreted as a by-passed oil zone requiring further well intervention. If two 3D reservoir models are created, using the fractal prediction and current day resistivity logs, the difference model will create a swept and by-passed map of the reservoir.

The thin bed at 145 ft shows the correct Sw as interpreted from the fractal function where the resistivity log over estimates Sw. There are bed boundary effects shown in the Sw computed from the resistivity log at 180 ft that are not shown on the Sw computed from the fractal function.

COMPARISON BETWEEN CORE AND LOG DERIVED FRACTAL SWH FUNCTIONS

Data from eleven UK North Sea fields (250 wells) were used in this study (Gagnon 2008). Electrical logs and conventional core (porosity and permeability) data were available from all eleven fields together with thin section and capillary pressure data.

The fields with electrical log data used in the study are listed in Table 1. They were selected as they represent a range of reservoir fluids, depositional environments. The fields included both gas and oil accumulations in different types of clastic reservoirs from different depositional environments. The broad spectra of fields were chosen to assess the robustness of the fractal function. Table 1 lists the fields, their fluid type and depositional environment.

Field	Fluid	Type	Porosity (pu)	Perm (mD)
	Gas	Permian Fluvial	9	0.2
	Oil	M. Jurassic Deltaic	13	3
	Oil	Devonian Lacustrine	14	7
	Gas	Permian Aeolian	14	0.9
	Oil	Palaeocene Turbidite	20	21
	Gas	Permian Aeolian	20	341
	Gas Condensate	L. Cretaceous Turbidite	24	847
	Oil	U. Jurassic Turbidite	21	570
	Oil	Palaeocene Turbidite	21	24
	Oil	Palaeocene Turbidite	22	27
	Gas	Palaeocene Turbidite	32	2207

Table 1: Fields used in the Study

The poroperm distribution for the eleven fields with log and core data is shown in Figure 34, where average permeability increases with average porosity as expected. Average permeability spans four logarithmic cycles: from 0.1 mD to 2 Darcies. Porosities range from 8 to 32 Porosity Units (p.u.).

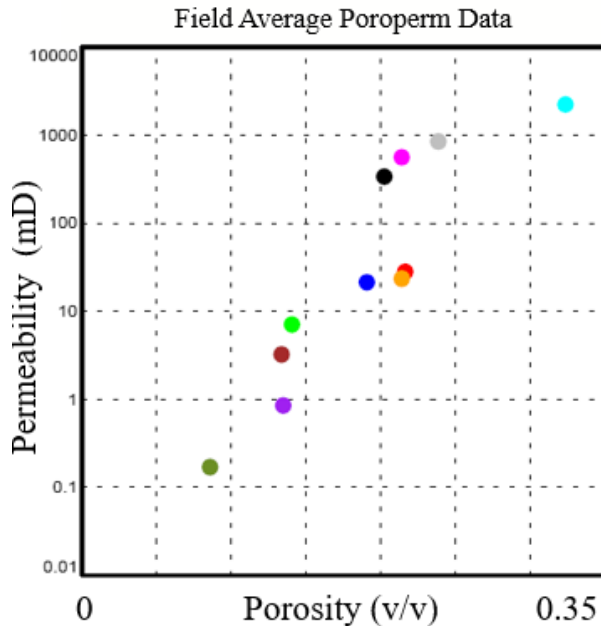


Figure 34: Average Porosity and Permeability for the Study Wells

A Fractal Function was determined *separately* from electrical log and the core data. The BVW for each well was calculated as the product of the water saturation and porosity curves. This was plotted against the height above the FWL. Only data away from conductive bed boundaries were included to minimise the effect of shoulder bed effects on the resistivity logs.

The Fractal Functions were calculated by plotting the logarithm (base 10) of BVW (x-axis) against the logarithm of the true vertical height (y-axis) above the FWL. Then a free linear regression (XonY) was used to compute the Fractal Function parameters. These fractal functions are shown by Figure 35.

The logarithmic scales plot of BVW against height above the FWL is shown in Figure 36. It is noticeable that all the fields share a similar 'b' parameter (slope) and the main difference between the SwH Functions is due to the variation of 'a' (intercept) between the fields.

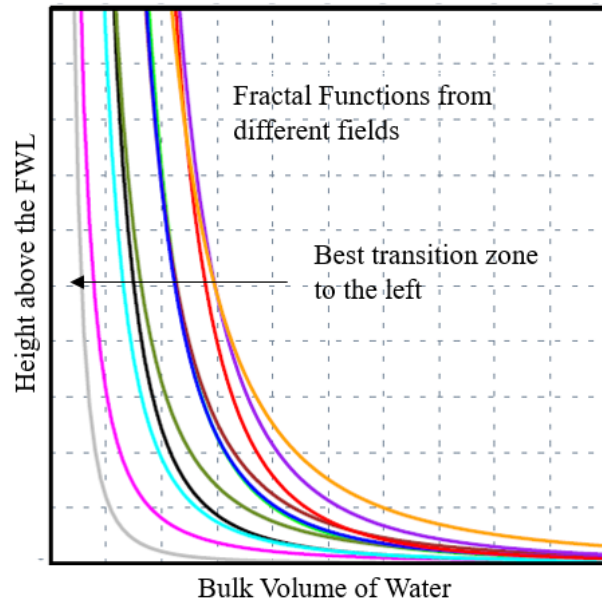


Figure 35: Fractal Functions for the study fields

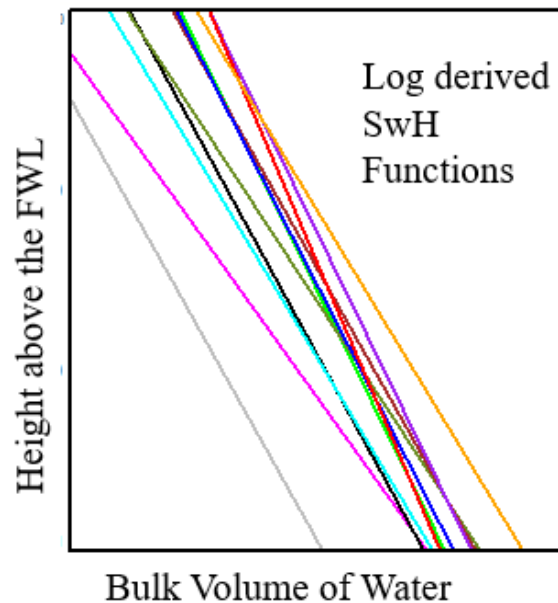


Figure 36: Fractal Functions on log-log Scales

The 'quality' of a reservoir is given by its value of water saturation at a certain height above FWL for a given porosity: with a lower Sw being considered the better-quality reservoir. The quality of a reservoir can be defined by the value of its 'a' parameter. Figure 35 shows reservoir quality increasing towards the bottom-left corner of the cross-plot. Notice that the parameter 'a' varies much more between these fields compared to the parameter 'b'.

The Fractal Functions derived from the core data from the same fields is shown by Figure 37. The core data are plotted against capillary pressure which is interchangeable with the height above the FWL as shown by Equation 12.

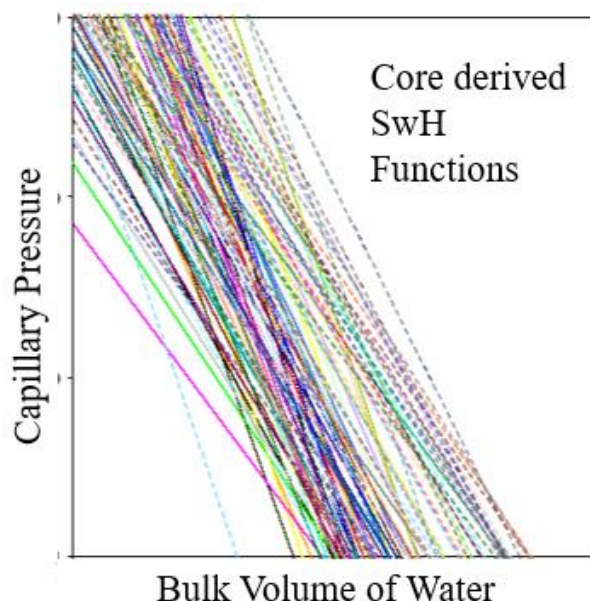


Figure 37: Core Derived Fractal Functions

Figure 36 shows the fractal function derived from the electrical logs using data between the FWL and the top of the reservoir for each field. Figure 37 shows the fractal function derived from the core data on the scale of a core plug (a few inches). As the functions agree this supports the fractal nature of pore geometry of these reservoirs.

UPSCALING WATER SATURATIONS

As Sw-Height functions (SwH) are used to initialize the 3D reservoir model, it is essential that the SwH predicted water saturations upscale accurately from ½ foot log or core scale to the cell size of the reservoir model. This is done by integrating the Sw-Height function.

Unlike other parameters, such as porosity, water saturation must be pore volume averaged as shown by equation 19.

$$\overline{Sw} = \frac{(\overline{\Phi_1 Sw_1} + \overline{\Phi_2 Sw_2})}{(\overline{\Phi_1} + \overline{\Phi_2})}$$

Equation 19

Where:

\overline{Sw} = average water saturation

$\overline{\Phi}$ = average porosity

$\overline{\Phi Sw}$ = average bulk volume of water

Average porosity is determined by the sum of the porosities together divided by their number. However, Sw must be pore volume weighted, which is the same as averaging BVW, the product of porosity and water saturation. Integration works for BVW functions but not for Sw functions. Worthington (2002) recommends using BVW functions as BVW is implicit in this equation.

CONCLUSIONS

We have determined from petrophysical first principles a fractal derived water saturation vs. height function to be used in reservoir modelling. The function has been shown to accurately describe the hydrocarbon and water distribution throughout the reservoir. This function can be derived from electrical log and/or core data using linear regression and is simply applied in the reservoir 3D model.

The fractal function is independent of rock characteristics such as facies type, porosity and permeability. This function can be used to determine a reservoir's hydrocarbon distribution, the field's free water level, local hydrocarbon water contacts, the net reservoir cut-off, the shape of the transition zone and the irreducible water saturation. The function can be derived from just two good electrical log or core data points and doesn't require the resistivity log to be corrected for bed boundaries, thin beds or conductive shales. As the function is based on BVW, it upscales correctly when integrated.

The electrical logs and core data give the same function which confirms the fractal nature of hydrocarbon bearing reservoirs. Fractal SwH Functions can therefore be used to quality control core and electrical logs against each other, and justifies using small core plugs to derive a water saturation vs. height function on the scale of a reservoir.

ACKNOWLEDGEMENTS

The authors would like to thank Baker Hughes for the use of their data and resources, and to the University of Leeds, School of Earth and Environment, for their guidance.

REFERENCES

AL-ZAINALDIN, S., GLOVER, P.W.J., LORINCZI, P. 2016. Synthetic Fractal Modelling of Heterogeneous and Anisotropic Reservoirs for Use in Simulation Studies: Implications on Their Hydrocarbon Recovery Prediction Transp Porous Med DOI 10.1007/s11242-016-0770-3

ANGULO, R., V. ALVARADO, V., GONZALEZ, H., 1992. Fractal Dimensions from Mercury Intrusion Capillary Tests R.F. SPE 23695

CUDDY, S., 1993. The Fractal function - a simple, convincing model for calculating water saturations in Southern North Sea gas fields: Transactions of the 34th Annual Logging Symposium of the SPWLA, H1-17, Calgary, Canada., 1993, BP Exploration.

GAGNON, D., CUDDY, S., CONTI, F., LINDSAY, C., 2008. The effect of pore geometry on the distribution of reservoir fluids in U.K. North Sea oil and gas fields. Transaction of the 49th Annual Logging Symposium of the SPWLA, May 25-28, 2008.

KATZ, A.J., THOMPSON, A.H. 1985 Fractal sandstone pores: implications for conductivity and pore formation. Phys. Rev. Lett. Phys. Rev. Lett. **54**, 1325-1328

KAY, S., CUDDY, S., 2002. Innovative Use of Petrophysics in Field Rehabilitation, with Examples from the Heather Field. Petroleum Geoscience, v.8, no 4, pp. 317-325.

LEVERETT, M.C., 1941. Capillary behaviour in porous solids: Trans AIME, Vol. 142.

LI, K., HORN, R., 2004. Universal Capillary Pressure and Relative Permeability Model from Fractal Characterization of Rock. Proceedings, Twenty-Ninth Workshop on Geothermal Reservoir Engineering Stanford University, Stanford, California, January 26-28, 2004

LOZADA-ZUMAETA et al., 2012. Distribution of petrophysical properties for sandy-clayey reservoirs by fractal interpolation. Nonlinear Process. Geophys. 19, 239-250

MANDAL, D., et al. 2006. Use of fractal geometry for determination of pore scale rock heterogeneity. International Conference & Exposition on Petroleum Geophysics, Kolkata.

MANDELBROT, B.B., 1977. Fractals: Form, Chance, and Dimension. W.H. Freeman, San Francisco.

TURCOTTE, D.L., 1997. Fractals and Chaos in Geology and Geophysics. Cambridge University Press, Cambridge.

WORTHINGTON, P.F., LOVELL, M. and PARKINSON, N., 2002. Application of saturation-height functions in integrated reservoir description: AAPG Methods in Exploration Series, 13, pp. 89.

ABOUT THE AUTHOR

Steve Cuddy is currently a Principal Petrophysicist with Baker Hughes. He is Honorary Research Fellow at Aberdeen University where he holds a PhD in petrophysics. He also holds a BSc in physics and a BSc in astrophysics and philosophy. He has 40 years industry experience in formation evaluation and reservoir description. He has authored several SPE and SPWLA papers and carried out more than 200 reservoir studies.



NOMENCLATURE AND DEFINITIONS

a	Fractal Function constant (Line Intercept)
b	Fractal Function constant (Line Gradient)
BVW	Bulk volume of water (v/v). The product of S_w and Φ .
D	Fractal dimension
FWL	Free water level (feet). Depth of zero capillary pressure
g	Acceleration of gravity
H	Height above the FWL (feet)
HWC	Hydrocarbon water contact
N	The number of the units (with a side of r) that will to <i>fill</i> entire object.
P_c	Capillary pressure (psi)
Φ	Effective porosity (PU)
S_w	Water saturation (%)
S_{wH}	Water saturation vs. height function
S_{wirr}	Irreducible water saturation
r	Capillary radius
σ	Interfacial tension
θ	Contact angle
ρ_w	Water density
ρ_o	Oil density

